


Observation of Squeezed States of Light in Higher-Order Hermite-Gaussian Modes with a Quantum Noise Reduction of up to 10 dB

Joscha Heinze¹, Benno Willke², and Henning Vahlbruch¹

Max-Planck-Institut für Gravitationsphysik (Albert-Einstein-Institut) and Leibniz Universität Hannover, 30167 Hannover, Germany

 (Received 15 October 2021; accepted 26 January 2022; published 25 February 2022)

Mirror thermal noise will be a main limitation for the sensitivities of the next-generation ground-based gravitational-wave detectors (Einstein Telescope and Cosmic Explorer) at signal frequencies around 100 Hz. Using a higher-order spatial laser mode instead of the fundamental mode is one proposed method to further mitigate mirror thermal noise. In the current detectors, quantum noise is successfully reduced by the injection of squeezed vacuum states. The operation in a higher-order mode would then require the efficient generation of squeezed vacuum states in this mode to maintain a high quantum noise reduction. In our setup, we generate continuous-wave squeezed states at a wavelength of 1064 nm in the fundamental and three higher-order Hermite-Gaussian modes up to a mode order of 6 using a type-I optical parametric amplifier. We present a significant milestone with a quantum noise reduction of up to 10 dB at a measurement frequency of 4 MHz in the higher-order modes and pave the way for their usage in future gravitational-wave detectors as well as in other quantum noise limited experiments.

DOI: [10.1103/PhysRevLett.128.083606](https://doi.org/10.1103/PhysRevLett.128.083606)

During the third joint observation run in 2019 and 2020, the sensitivities of the gravitational-wave detectors Advanced LIGO and Advanced Virgo were mainly limited by quantum noise and mirror thermal noise in the frequency range around 100 Hz [1,2]. Squeezed vacuum states were injected into the detectors' output ports to effectively reduce the quantum shot noise by about 3 dB and low-loss optical coatings were used to mitigate the mirror thermal noise. The prospects for the future ground-based detectors Einstein Telescope (ET) and Cosmic Explorer (CE) include major advances in the quantum noise reduction with an envisaged effective squeezing level of 10 dB [3,4]. Mirror thermal noise is likely to become one of the dominating factors in the overall noise budget of ET and CE, even though advances regarding this noise source are expected as well. A proposal for its further mitigation, which is currently beyond the baseline of the ET and CE designs, is the usage of higher-order spatial laser modes instead of the fundamental Gaussian TEM_{0,0} mode [5]. After several experiments revealed that astigmatism constitutes a large challenge for higher-order Laguerre-Gaussian modes [6–9], the research focus switched to Hermite-Gaussian (HG) modes [10–12]. Here, one remaining question is whether squeezed vacuum states can be efficiently generated in these higher-order modes to maintain a high quantum noise reduction.

Other important fields of application are, e.g., quantum imaging [13] and quantum information, where entangled higher-order modes can convey several independent channels for communication and spatial sensing [14].

The generation of continuous-wave squeezed vacuum states in the TEM_{0,0} mode for gravitational-wave detectors is based on cavity-enhanced second harmonic generation (SHG) and subsequent parametric down-conversion in an optical parametric amplifier (OPA), where both processes are conducted in nonlinear crystals [15,16]. This scheme can be adapted to higher-order spatial modes in two distinct ways. In the indirect method, the squeezed states are first generated in the TEM_{0,0} mode which is then converted into a higher-order mode. While the generation of squeezed states in the TEM_{0,0} mode can be performed with high efficiency [17], currently available mode conversion techniques add optical loss to the squeezed field due to absorption and the partial conversion into unwanted modes [10,18]. Hence, the results for this indirect method have remained below 3 dB of quantum noise reduction so far [19].

In the second method, the OPA directly modifies the quantum statistic of the higher-order mode without an intermediate TEM_{0,0} squeezing. Here, no spatial manipulation of the squeezed field is required, which renders this method the theoretically more efficient one. 3 dB have, however, also been the upper limit for the direct generation of squeezing and entanglement so far [20,21].

We chose to directly generate squeezed states in the Hermite-Gaussian modes HG_{1,1}, HG_{2,2}, and HG_{3,3} to compare their quantum noise reduction (squeezing level), pump power, optical loss budget, and phase noise to the squeezing process of the TEM_{0,0} mode in one setup using the same type-I OPA. To efficiently generate squeezed states

directly in a higher-order mode via parametric down-conversion, the harmonic pump field has to be spatially adapted to the squeezed mode. The optimum pump field is characterized by a minimum threshold power—which, in the absence of phase noise, corresponds to the pump power for which the highest squeezing level is obtained—and can be derived from the following dependence of the threshold power P_{thr} on the squeezed field A_{sqz} and pump field A_p [22]:

$$P_{\text{thr}} \propto \left| \int [\mathbf{A}_{\text{sqz}}^*(\mathbf{r})]^2 \mathbf{A}_p(\mathbf{r}) dV \right|^{-2}, \quad (1)$$

where \mathbf{A}_{sqz} and \mathbf{A}_p are the corresponding three-dimensional amplitude distributions and the integral is evaluated over the volume of the nonlinear medium. This volume integral can be split up into a surface integral, evaluated over the cross-section of the nonlinear medium, and a line integral, evaluated along the propagation axis. The surface integral tells us that the pump field for the mode $\text{HG}_{m,n}$ can, in general, be any arbitrary normalized superposition of the harmonic HG modes which have a nonzero spatial overlap with $\text{HG}_{m,n}^2$:

$$A_p(\text{HG}_{m,n}) = \sum_{k=0}^m \sum_{j=0}^n a_{2k,2j} \text{HG}_{2k,2j}^h, \quad (2)$$

where $a_{2k,2j}$ are complex-valued coefficients and the superscript h denotes the harmonic modes which have a reduced waist size ($\omega_0^h = \omega_0/\sqrt{2}$) and twice the frequency. The line integral assesses the phase matching between the squeezed and pump field. These two integrals are typically not maximized by the same pump field such that the optimum pump field has to be derived as a trade-off which additionally depends on the focusing parameter [23].

We generate the pump field for the higher-order HG modes via the second harmonic generation of the $\text{TEM}_{0,0}$ mode and one spatial light modulator (SLM, type: Hamamatsu LCOS) which then converts the harmonic $\text{TEM}_{0,0}$ mode into the used pump field. This SLM type only modulates the transverse phase distribution of the incoming field, not the intensity distribution. With this limited influence, it cannot produce any arbitrary superposition such that we simplified our considerations about the optimum pump field to only one single pump mode per squeezed mode. If the harmonic modes in Eq. (2) are analyzed individually, $\text{HG}_{2m,2n}^h$ provides the highest spatial overlap to $\text{HG}_{m,n}^2$ as well as the best phase matching. Hence, we use the harmonic $\text{HG}_{2m,2n}^h$ mode to directly generate squeezed states in the $\text{HG}_{m,n}$ mode. Assuming this choice of spatial pump mode, Table I shows the threshold powers calculated with Eq. (1).

For gravitational-wave detectors, the OPAs are typically operated as a dual-resonant cavity, where the pump and squeezed field are simultaneously resonant and the pump

TABLE I. Calculated threshold power P_{thr} for the different $\text{HG}_{m,n}$ modes, when pumped by the $\text{HG}_{2m,2n}^h$ mode, in the same OPA. P_{thr} is normalized to 1 for the $\text{TEM}_{0,0}$ ($=\text{HG}_{0,0}$) mode.

m, n	0,0	1,1	2,2	3,3
P_{thr}	1.0	4.0	7.1	10.2

field is used for the OPA length stabilization [15,16]. In our experiment, the squeezed mode and the corresponding pump mode do, however, not share the same mode order (except for the $\text{TEM}_{0,0}$ mode squeezing) and are, in general, nondegenerate in a cavity. This does not render the typical OPA design impossible, but given that we aimed to compare four modes with the same OPA cavity, we chose a single-resonant cavity design instead, where the squeezed field is resonating while the in-coupling mirror is completely transmissive for the pump field. We then use an OPA control field at the fundamental frequency in the spatial mode which is squeezed to stabilize the OPA length via the Pound-Drever-Hall scheme. About 2% of this control field is transmitted by the OPA cavity and causes a coherent amplitude in the squeezed field. We thus generate bright squeezed states in the respective HG modes. Furthermore, we need an additional control loop to stabilize the relative phase between the pump field and this OPA control field to simultaneously stabilize the measured squeezing quadrature angle.

Our hemilithic linear OPA cavity contains a periodically poled potassium titanyl phosphate (PPKTP) crystal which measures $1.0 \times 2.0 \times 9.3$ mm in the x , y , and z (propagation) direction. The curved crystal face serves as a highly reflective end mirror, $R_{\text{end},1064 \text{ nm}} > 99.96\%$ and $R_{\text{end},532 \text{ nm}} = 99.9\%$, while the plane face is antireflective coated for both wavelengths. The nominal reflectivities of the in-coupling mirror are $R_{\text{in},1064 \text{ nm}} = 92\%$ and $R_{\text{in},532 \text{ nm}} < 0.2\%$ such that the OPA's half width at half maximum (bandwidth) is about 25 MHz. The radii of curvature are $R_{c,\text{in}} = 25$ mm and $R_{c,\text{end}} = 12$ mm, setting the waist of the squeezed field's eigenmodes to about $33 \mu\text{m}$ in radius near the crystal center. A peltier element stabilizes the crystal temperature via a control loop and is used to optimize the phase matching. The SHG cavity has the same design besides a reflectivity of the in-coupling mirror of $R_{\text{in},1064 \text{ nm}} = 90\%$.

Figure 1 shows a schematic of our experimental setup. It is operated with a 2 W nonplanar ring laser (NPRO) continuously emitting light in the $\text{TEM}_{0,0}$ mode at a wavelength of 1064 nm. The quarter-wave plate optimizes the linear polarisation and the half-wave plate in combination with the Faraday isolator (FI) determines the power injected into the whole experiment. A phase modulation at a frequency of 120 MHz, driven by the rf-generator (rf), is imprinted by the electro-optical modulator (EOM) for the length stabilization of the SHG cavity, and the mode cleaner (MC) via the Pound-Drever-Hall scheme. The light

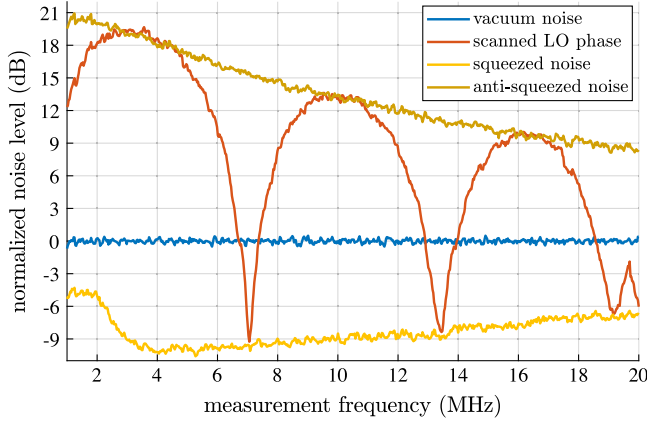


FIG. 3. Measurement result for the $HG_{1,1}$ mode at a total harmonic power of 610 mW. LO: local oscillator field. Resolution bandwidth: 300 kHz, video bandwidth: 300 Hz, electronic dark noise (not shown): about -25 dB over full span and not subtracted from the data.

power than expected from Table I to achieve the same squeezing levels as the $TEM_{0,0}$ mode because we do not filter the harmonic field downstream SLM_2 and because the mode matching of the pump mode to the OPA cavity rapidly decreases with increasing mode order [24]. We estimate that the pump field effectively consists of the intended pump mode to only 20% to 30%, at most, and distinguish between the effective pump power and the measured “total harmonic OPA pump power” (short: total harmonic power). Nevertheless, we only measure vacuum or squeezed noise in the intended mode due to the mode-filtered local oscillator.

We also compare our measurement results to a theoretical model. Below threshold and in the absence of phase noise, the squeezed ($-$) and antisqueezed ($+$) quadrature variances of the squeezed field leaving the OPA cavity can be computed as [25]

$$\Delta^2 \hat{X}_{+,-} = 1 \pm \eta_{\text{det}} \frac{4\sqrt{P/P_{\text{thr}}}}{(1 \mp \sqrt{P/P_{\text{thr}}})^2 + 4(\frac{2\pi f}{\gamma})^2}, \quad (3)$$

where η_{det} is the detection efficiency, P is the total harmonic power as explained above, P_{thr} now relates to the total harmonic power, f is the measurement frequency and

TABLE II. Maximum squeezing levels together with the corresponding antisqueezing level and the total harmonic power.

	Maximum squeezing level (dB)	Corresponding antisqueezing level (dB)	Corresponding total harmonic power (mW)
$TEM_{0,0}$	11.8(3)	19.9(3)	41.8(4)
$HG_{1,1}$	10.1(3)	17.9(3)	608(6)
$HG_{2,2}$	7.5(3)	10.7(3)	1005(10)
$HG_{3,3}$	4.5(3)	6.4(3)	1000(10)

$\gamma = c(T + L)/l$ is the cavity decay rate with the speed of light c , the in-coupling mirror’s power transmissivity T , the round-trip loss L and the round-trip optical path length l . The effect of fluctuations in the relative phase (phase noise) between the local oscillator field and the squeezed field can be included by assuming that the homodyne detector measures at a phase offset θ :

$$V_{+,-} = \Delta^2 \hat{X}_{+,-} \cos^2 \theta + \Delta^2 \hat{X}_{-,+} \sin^2 \theta. \quad (4)$$

We varied the parameters η_{det} , θ and P_{thr} to obtain the best match between this theoretical model and our measurement results (solid lines in Fig. 2). The fitted parameters are shown in Table III apart from the threshold power because its value is misleading due to the discrepancy between the effective pump power and the total harmonic power.

The fitted detection efficiencies are in good agreement with our expectations which are derived from the expected total optical loss. Included in the total optical loss are the OPA escape efficiency $T/(T + L) = 99.0(5)\%$, the quantum efficiency of the homodyne detector’s photodiodes [99.0(5)%] and loss from optics in the path of the squeezed field [0.4(2)%]. We assume these three values to be equal for the four modes. Finally, the homodyne detector only measures the quantum noise reduction in the fraction of the squeezed field which is mode matched to the local oscillator field. The corresponding mode-matching term for the expected detection efficiency is equal to the square of the measured homodyne contrast which can also be found in Table III. A high homodyne contrast becomes more challenging with increasing mode order [24].

The effect of phase noise only becomes clearly visible in the regime of high antisqueezing. For the $HG_{2,2}$ and $HG_{3,3}$ mode, the available harmonic power was not sufficient to reach this regime. In the range of the expected detection efficiency, our fitting routine did not resolve phase noise below 50 mrad for the $HG_{2,2}$ mode such that the generated phase noise values are not conclusive. For the $HG_{3,3}$ mode, the harmonic power did not suffice to take enough data points for a reasonable fit in Fig. 2, at all. Our $HG_{3,3}$ measurement can be explained with a detection efficiency

TABLE III. Measured homodyne contrast and the expected detection efficiency. The fitted detection efficiency and phase noise are the parameters used to obtain the theoretical curves in Fig. 2. [not conclusive (n.c.).]

	Measured homodyne contrast (%)	Expected detection efficiency (%)	Fitted detection efficiency (%)	Fitted phase noise (mrad)
$TEM_{0,0}$	98.5(5)	94.6(12)	94.4(3)	4 (≤ 10)
$HG_{1,1}$	98.0(5)	93.6(12)	92.7(3)	16 (≥ 15)
$HG_{2,2}$	96.0(5)	89.8(12)	89.0(3)	n.c.
$HG_{3,3}$	95.5(5)	88.8(12)	n.c.	n.c.

of 87(6)% and a phase noise of 80(70) mrad such that both parameters cannot be properly inferred from the theoretical model.

There is, however, a clear difference of at least 5 mrad in the fitted phase noise of the TEM_{0,0} and HG_{1,1} mode. Since the only differences in the setups for these two modes are the two SLMs, we expect their discrete operation which works with a frame repetition rate of 60 Hz to be the most likely cause for the higher phase noise.

Figure 3 shows one HG_{1,1} full-span measurement where we achieved a squeezing level of 10 dB at 4 MHz for a total harmonic power of about 610 mW. For the squeezing and antisqueezing curves, we stabilized the relative phase between the squeezed field and local oscillator field, accordingly. Both curves decrease towards higher frequencies in agreement with effects due to the OPA bandwidth. For the “scanned LO phase” curve, we scanned this relative phase over more than two cycles during the scan time of the spectrum analyzer. This results in the oscillation between the squeezing and antisqueezing levels. The increased noise in the squeezing curve at low frequencies is the residual technical laser noise of the fraction of the OPA control field which is transmitted through the OPA and also measured by the balanced homodyne detector.

In conclusion, we demonstrated the general feasibility of experiments which require a high quantum noise reduction in higher-order spatial modes. To our knowledge, this is the first time that squeezing levels above 3 dB are reported for any higher-order mode. Besides the 12 dB in the TEM_{0,0} mode, we thus present a significant new benchmark with 10 dB in the HG_{1,1} mode, 7.5 dB in the HG_{2,2} mode and 4.5 dB in the HG_{3,3} mode, where the last two results were primarily limited by the available pump power. The fitted detection efficiencies are in good agreement with our expected optical loss budgets and the spatial light modulators used to generate the higher-order modes most likely increased the phase noise of the higher-order mode measurements. The adaptation of our scheme to other frequency bands (e.g., the audio band for gravitational-wave detectors) and the generation of squeezed vacuum states are now technical steps which can be carried out in the same way as for the TEM_{0,0} mode [26].

Funded by the Deutsche Forschungsgemeinschaft (DFG, German Research Foundation) under Germany’s Excellence Strategy EXC-2123 QuantumFrontiers 390837967.

*joscha.heinze@aei.mpg.de

- [1] A. Buikema, C. Cahillane, G. L. Mansell, C. D. Blair, R. Abbott, C. Adams, R. X. Adhikari, A. Ananyeva, S. Appert, K. Arai *et al.*, Sensitivity and performance of the advanced LIGO detectors in the third observing run, *Phys. Rev. D* **102**, 062003 (2020).
- [2] C. Nguyen, Status of the Advanced Virgo gravitational-wave detector, [arXiv:2105.09247](https://arxiv.org/abs/2105.09247).
- [3] ET Steering Committee, ET Design Report Update 2020, <http://www.et-gw.eu/index.php/relevant-et-documents> (2020).
- [4] D. Reitze, R. X. Adhikari, S. Ballmer, B. Barish, L. Barsotti, G. Billingsley, A. D. Brown, Y. Chen, D. Coyne, R. Eisenstein *et al.*, Cosmic Explorer: The U.S. contribution to gravitational-wave astronomy beyond LIGO, *Bull. Am. Astron. Soc.* **51**, 035 (2019), <https://inspirehep.net/literature/1743201>.
- [5] J.-Y. Vinet, Thermal noise in advanced gravitational wave interferometric antennas: A comparison between arbitrary order Hermite and Laguerre Gaussian modes, *Phys. Rev. D* **82**, 042003 (2010).
- [6] B. Sorazu, P. J. Fulda, B. W. Barr, A. S. Bell, C. Bond, L. Carbone, A. Freise, S. Hild, S. H. Huttner, J. Macarthur, and K. A. Strain, Experimental test of higher-order Laguerre-Gauss modes in the 10m Glasgow prototype interferometer, *Classical Quantum Gravity* **30**, 035004 (2013).
- [7] T. Hong, J. Miller, H. Yamamoto, Y. Chen, and R. Adhikari, Effects of mirror aberrations on Laguerre-Gaussian beams in interferometric gravitational-wave detectors, *Phys. Rev. D* **84**, 102001 (2011).
- [8] C. Bond, P. Fulda, L. Carbone, K. Kokeyama, and A. Freise, Higher order Laguerre-Gauss mode degeneracy in realistic, high finesse cavities, *Phys. Rev. D* **84**, 102002 (2011).
- [9] J. Heinze, H. Vahlbruch, and B. Willke, Frequency-doubling of continuous laser light in the Laguerre-Gaussian modes LG_{0,0} and LG_{3,3}, *Opt. Lett.* **45**, 5262 (2020).
- [10] S. Ast, S. Di Pace, J. Millo, M. Pichot, M. Turconi, N. Christensen, and W. Chaibi, Higher-order Hermite-Gauss modes for gravitational waves detection, *Phys. Rev. D* **103**, 042008 (2021).
- [11] A. W. Jones and A. Freise, Increased sensitivity of higher-order laser beams to mode mismatches, *Opt. Lett.* **45**, 5876 (2020).
- [12] L. Tao, A. Green, and P. Fulda, Higher-order Hermite-Gauss modes as a robust flat beam in interferometric gravitational wave detectors, *Phys. Rev. D* **102**, 122002 (2020).
- [13] M. T. L. Hsu, W. P. Bowen, N. Treps, and P. K. Lam, Continuous-variable spatial entanglement for bright optical beams, *Phys. Rev. A* **72**, 013802 (2005).
- [14] M. Lassen, V. Delaubert, J. Janousek, K. Wagner, H.-A. Bachor, P. K. Lam, N. Treps, P. Buchhave, C. Fabre, and C. C. Harb, Tools for Multimode Quantum Information: Modulation, Detection, and Spatial Quantum Correlations, *Phys. Rev. Lett.* **98**, 083602 (2007).
- [15] M. Mehmet and H. Vahlbruch, The squeezed light source for the Advanced Virgo detector in the observation run O3, *Galaxies* **8**, 79 (2020).
- [16] M. Tse, H. Yu, N. Kijbunchoo, A. Fernandez-Galiana, P. Dupej, L. Barsotti, C. D. Blair, D. D. Brown, S. E. Dwyer, A. Effler *et al.*, Quantum-enhanced Advanced LIGO detectors in the era of gravitational-wave astronomy, *Phys. Rev. Lett.* **123**, 231107 (2019).
- [17] H. Vahlbruch, M. Mehmet, K. Danzmann, and R. Schnabel, Detection of 15 dB of Squeezed States of Light and their Application for the Absolute Calibration of Photoelectric Quantum Efficiency, *Phys. Rev. Lett.* **117**, 110801 (2016).
- [18] L. Carbone, C. Bogan, P. Fulda, A. Freise, and B. Willke, Generation of High-Purity Higher-Order Laguerre-Gauss

- Beams at High Laser Power, *Phys. Rev. Lett.* **110**, 251101 (2013).
- [19] L. Ma, H. Guo, H. Sun, K. Liu, B. Su, and J. Gao, Generation of squeezed states of light in arbitrary complex amplitude transverse distribution, *Photonics Res.* **8**, 001422 (2020).
- [20] M. Lassen, V. Delaubert, C. C. Harb, P. K. Lam, N. Treps, and H.-A. Bachor, Generation of squeezing in higher order Hermite-Gaussian modes with an optical parametric amplifier, *J. Eur. Opt. Soc.* **1**, 06003 (2006).
- [21] J. Guo, C. Cai, L. Ma, K. Liu, H. Sun, and J. Gao, Higher order mode entanglement in a type II optical parametric oscillator, *Opt. Express* **25**, 4985 (2017).
- [22] G. Boyd and D. A. Kleinmann, Parametric interaction of focused Gaussian light beams, *J. Appl. Phys.* **39**, 3597 (1968).
- [23] J. Heinze, H. Vahlbruch, and B. Willke, Numerical analysis of $LG_{3,3}$ second harmonic generation in comparison to the $LG_{0,0}$ case, *Opt. Express* **28**, 35816 (2020).
- [24] L. Tao, J. Kelley-Derzon, A. C. Green, and P. Fulda, Power coupling losses for misaligned and mode-mismatched higher-order Hermite-Gauss modes, *Opt. Lett.* **46**, 2694 (2021).
- [25] E. S. Polzik, J. Carri, and H. J. Kimble, Atomic spectroscopy with squeezed light for sensitivity beyond the vacuum-state limit, *Appl. Phys. B* **55**, 279 (1992).
- [26] H. Vahlbruch, S. Chelkowski, B. Hage, A. Franzen, K. Danzmann, and R. Schnabel, Coherent Control of Vacuum Squeezing in the Gravitational-Wave Detection Band, *Phys. Rev. Lett.* **97**, 011101 (2006).